Controller design for enhancement position accuracy of a rigid-flexible links robot by using particle warm optimization algorithm

Thiết kế hệ điều khiển nâng cao độ chính xác vị trí của hệ rô bốt có khâu cứng và khâu đàn hồi ứng dụng thuật toán tối ưu bầy đàn

Bien Duong Xuan*, My Chu Anh
Military Technical Academy
**Email: xuanbien82@yahoo.com*

Abstract

Keywords:

Controller design; Flexible robot; Condition boundary; Position accuracy; PSO.

This paper presents the results of controller designing for enhancement position accuracy of two-link flexible robot which motions on planar plane. The first link is rigid with rotational joint and the second link is flexible and slides in translational joint which fixed mounted the end point of link 1. Finite element method (FEM) and Lagrange equations are used dynamic modeling the system. The length of work part of flexible link 2 is continuously changed and drags on changing of conditions boundary. These factors are many challengers in modeling, solving nonlinear differential equations (DE) of motion and designing controller. Elastic displacements at the end-effector directly effect on position accuracy of robot. The extended PID control is designed to reduce effecting of these displacement. The parameters of PID control are optimized by using Particle Swarm Optimization (PSO) algorithm. The solving technique with changing conditions boundary also clealy present.

Tóm tắt

Từ khóa:

Thiết kế hệ điều khiển; Rô bốt đàn hồi; Điều kiện biên; Độ chính xác vị trí; Thuật toán bầy đàn.

Bài báo này trình bày kết quả nghiên cứu thiết kế hệ điều khiển nâng cao độ chính xác vị trí cho hệ rô bốt có 2 khâu nối tiếp chuyển động trong mặt phẳng. Rô bốt có khâu 1 cứng chuyển động quay, khâu 2 đàn hồi và chuyển động trượt trong khớp tịnh tiến được gắn cố định vào điểm cuối của khâu cứng 1. Phương pháp phần tử hữu hạn kết hợp với hệ phương trình Lagrange loại 2 được sử dụng để mô hình hóa động lực học hệ rô bốt. Chiều dài làm việc của khâu đàn hồi 2 liên tục thay đổi theo thời gian kéo theo sự thay đổi liên tục của điều kiện biên. Những yếu tố này tạo ra sự phức tạp trong mô hình hóa động lực học, giải hệ phương trình vi phân (DE) phi tuyến và thiết kế điều khiển. Yếu tố chuyển vị đàn hồi ảnh hưởng rất lớn tới độ chính xác chuyển động của hệ. Hệ điều khiển PID được thiết kế với các thông số Ki, Kp, Kd được tối ưu bằng thuật toán bầy đàn (PSO) nhằm làm giảm, tiến tới triệt tiêu ảnh hưởng của yếu tố chuyển vị đàn hồi và nâng cao độ chính xác vị trí của điểm thao tác rô bốt. Kỹ thuật giải hệ phương trình vi phân chuyển động có điều kiện biên thay đổi liên tục cũng được trình bày cụ thể.

Received: 20/7/2018
Received in revised form: 12/9/2018
Accepted: 15/9/2018

1. INTRODUCTION

There are challengers in dynamic modeling and control flexible robot [1], [2], [3] because of mentioning effect of elastic displacement in motion. Lumped Parameters Method (LPM) [4], Assumed Modes Method (AMM) [5], [6], [7] and Finite Element Method (FEM) [8], [9], [10] are mostly used to dynamic model of flexible robot. Traditional and intelligent controller systems are applicated to control these types. However, simple, effective and suitable with real time controller always is the first selection of researchers. Most of the investigations on robot with elastic arms have been confined to robot with only revolute joints [1], [2], [3]. Combining such systems with translational joints enables these robots to perform manipulation tasks in a much larger workspace, more flexibility and more applications. Translational joint is also the popular joint to connect links in robot mechanism such as cylindrical robots. Few authors have studied the manipulator with only translational joint [5], [6]. A number of researches focused on the flexible manipulator with a link slides through a translational joint with a simultaneous rotational motion [8], [11], [12]. However, most of studies on type of sliding flexible link in translational joint have not clearly analyzed in conditions boundary and solving nonlinear differential equations with dynamic modeling using FEM. There are many researchers who focused on intelligent control system development to end-effectors control as Fuzzy Logic [13], Neural Network [14], PSO [15], Back-stepping [16] and Genetic Algorithm [9]. PSO was formulated by Edward and Kennedy in 1995. PSO algorithm is optimization technique by social behavior of bird flocking [15].

This paper forcus on controller designing for enhancement position accuracy of two-link flexible robot. The first link is rigid with rotational joint and the second link is flexible and slides in translational joint which fixed mounted the end point of link 1. Finite element method (FEM) and Lagrange equations are used dynamic modeling the system. The length of work part of flexible link 2 is continuously changed and drags on changing of conditions boundary. The solving technique with changing conditions boundary also clealy present. The extended PID control is designed to reduce effecting of these displacement. The parameters of PID control are optimized by using Particle Swarm Optimization (PSO) algorithm.

2. DYNAMIC MODELING

2.1. Dynamic equations

Considering the flexible robot with rotational/translational joints is shown in Fig.1. The coordinate system XOY is the fixed frame. Coordinate system $X_1O_1Y_1$ is attached to first point of rigid link 1. Coordinate system $X_2O_2Y_2$ is attached to the center of translational joint which is fixed mounted the end point of link 1. The rotational joint variable $\theta(t)$ is driven by $\tau(t)$ torque and translational joint $d(t)$ is driven by F force. Joints are assumed rigid. Link 1 is rigid. Link 2 is flexible and divided n elements. The length of link 2 is L_2 . The elements are assumed interconnected at certain points, known as nodes. Each element j, $j=1\div n$ has two nodes $(j,j+1)$. Each node of element j has 2 elastic displacement variables which are the flexural displacement (u_{2j-1},u_{2j+1}) and the slope displacements (u_{2j},u_{2j+2}), respectively. Element k is any element which slides through prismatic joint. Assumed that the length of prismatic joint is shorter than length of element k and without loss of generality, the elastic displacements at the node k are zero $\left(u_{2k-1}=u_{2k}=0\right)$ if these displacements are behind or inside prismatic joint (Fig. 2). This is the conditions boundary which are continuously changed by varying k value while solving differential equations. Defining the part in work is from element k to the end-effector point. We have

$$kl_e=L_2-d(t) \tag{1}$$

Index of element k must be integer value, so it can be taken integer part in Eq. (2)

$$k=\left\lfloor \frac{L_2-d(t)}{l_e} \right\rfloor \tag{2}$$

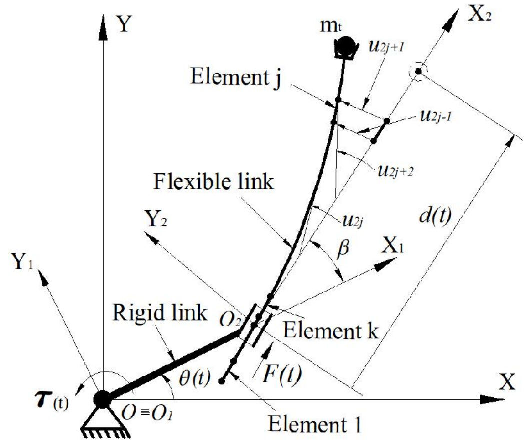

Fig. 1. Rigid-flexible links robot

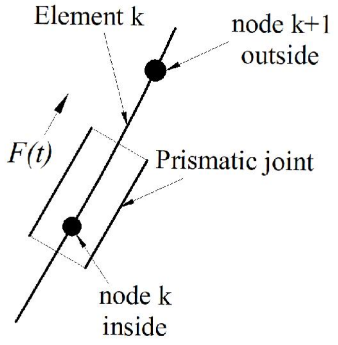

Fig. 2. Position of element k

The dynamic equation of motion relies on the Lagrange equations with Lagrange function $L=T-P$ given by

$$\frac{d}{dt}\left(\frac{\partial L}{\partial \dot{\mathbf{q}}}\right)^T-\left(\frac{\partial L}{\partial \mathbf{q}}\right)^T=\mathbf{Q}(t) \tag{3}$$

Where, T and P are the kinetic and potential energy of the system. Vector $\mathbf{Q}(t)=\left[\tau(t)\ F(t)\ 0..\ ..\ 0\ 0\right]^T$ is external generalized torque with rotational joint or force with translational joint acting along components of the generalized coordinate $\mathbf{q}(t)$**.** Assumed that robot motions in horizontal plane, effect of gravity is can be ignored. The equations of motion can be expressed as

$$\mathbf{M}(\mathbf{q})\ddot{\mathbf{q}}+\mathbf{C}(\mathbf{q},\dot{\mathbf{q}})\dot{\mathbf{q}}+\mathbf{K}\mathbf{q}=\mathbf{Q}(t) \tag{4}$$

Where, the Coriolis and centrifugal matrix is $\mathbf{C}$ which is correspondingly calculated as in [17]. The structural damping is ignored in this study. The generalized inertia matrix $\mathbf{M}$ and the stiffness matrix $\mathbf{K}$ are calculated by proposed assembly algorithm based on FEM theory. The size of matrices $\mathbf{M},\mathbf{K}$ and $\mathbf{C}$ is $(2n+4)\times(2n+4)$. All components of $\mathbf{M},\mathbf{K}$ and $\mathbf{C}$ are related to the elastic deformation of links and they will be determined in the generalized case. Considering element j of link 2, a point $\mathbf{r}_{2j}(x)$ represented in $X_2O_2Y_2$, where $0\le x\le l_e$ and $l_e = {}^{L_2}\!/_{n}$, can be computed as follows

$$\mathbf{r}_{2j}(x)=\left[(j-1)l_e-L_2+d(t)+x \;\; w_j(x) \;\; 0 \;\; 1\right]^T \tag{5}$$

Notice that $w_j(x)$ is the total elastic displacement of element j, $w_j(x)=\mathbf{N}_j(x)\mathbf{q}_j$; $\mathbf{N}_j(x)$ is the vector of the shape functions, $\mathbf{N}_j(x)=\left[\phi_1(x) \;\; \phi_2(x) \;\; \phi_3(x) \;\; \phi_4(x)\right]$; The computation of the shape functions is detailed in [usoro]; $\mathbf{q}_j$ is the vector of elastic displacements of the element j, $\mathbf{q}_j=\left[u_{2j-1} \;\; u_{2j} \;\; u_{2j+1} \;\; u_{2j+2}\right]^T$. Therefore, the point $\mathbf{r}_{2j}$ represented in XOY, can be expressed as

$$\mathbf{r}_{02j}=\mathbf{H}_{01}\mathbf{H}_{12}\mathbf{r}_{2j} \tag{6}$$

Where $\mathbf{H}_{01}$ and $\mathbf{H}_{12}$ are the homogeneous transformation matrices representing the transformation from $X_1O_1Y_1$ to XOY, and from $X_2O_2Y_2$ to $X_1O_1Y_1$, respectively. Notice that, because of the concept of homogeneous matrix used, the representation of vectors $\mathbf{r}_{2j}$, $\mathbf{r}_{02j}$ needs four components. However, in the following, only two first components of them are utilized to respect to the descriptions in the planar workspace. The kinetic energy of element j of link 2 is determined with $\mathbf{q}_{jg}=\left[\theta(t) \;\; d(t) \;\; u_{2j-1} \;\; u_{2j} \;\; u_{2j+1} \;\; u_{2j+2}\right]^T$ as [10]

$$T_{2j}=\frac{1}{2}\int_0^{l_e} m_2\dot{\mathbf{r}}_{02j}^T\dot{\mathbf{r}}_{02j}dx=\frac{1}{2}\dot{\mathbf{q}}_{jg}^T\mathbf{M}_j\dot{q}_{jg} \tag{7}$$

The total kinetic energy of link 2 is yielded as $T_e=\sum_{j=1}^{n}T_{2j}=\frac{1}{2}\dot{\mathbf{q}}^T\mathbf{M}_e\dot{\mathbf{q}}$. The matrix $\mathbf{M}_e$ is constructed from all the matrices $\mathbf{M}_j$. The total kinetic energy of the system is determined as $T=T_1+T_e+T_P=\frac{1}{2}\dot{\mathbf{q}}^T\mathbf{M}\dot{\mathbf{q}}$. Where T_1 and T_P are the kinetic energy of the first link and the payload which can be easily determined via the rigid model. Let E and I be Young's modulus and inertial moment of link 2, respectively. The elastic potential energy of element j, P_j, is computed as [10]

$$P_j=\frac{1}{2}\int_0^{l_e}EI\left(\frac{\partial^2 w_j(x,t)}{\partial x^2}\right)^T\left(\frac{\partial^2 w_j(x,t)}{\partial x^2}\right)dx=\frac{1}{2}\mathbf{q}_j^T\mathbf{K}_j\mathbf{q}_j \tag{8}$$

The total potential energy of the whole system is yielded as $P=\sum_{j=1}^{n}P_j=\frac{1}{2}\mathbf{q}^T\mathbf{K}\mathbf{q}$. The general stiffness matrix $\mathbf{K}$ is constructed from all matrices $\mathbf{K}_j$. Finally, substituting all matrices $\mathbf{M}$,$\mathbf{C}$ and $\mathbf{K}$ into Eq. (4) obtains the dynamic equations for the generalized model.

2.2. Boundary Conditions and solving DE technique

The displacements of its first node vanish $\left(u_{2k-1}=u_{2k}=0\right)$. Therefore, the $(2k+1)^{th}$ and the $(2k+2)^{th}$ rows and columns of the matrices $\mathbf{M},\mathbf{K}$ and $\mathbf{C}$ are continuously eliminated. The same positions of $\mathbf{q}(t)$ and $\mathbf{Q}(t)$ are eliminated, respectively. The size of matrices $\mathbf{M},\mathbf{K}$ and $\mathbf{C}$ is changed to $(2n+2)\times(2n+2)$ and the size of $\mathbf{q}(t)$ and $\mathbf{Q}(t)$ is $(2n+2)\times1$. The solving differential equations technique can be described as Fig. 3 in MATLAB/SIMULINK.

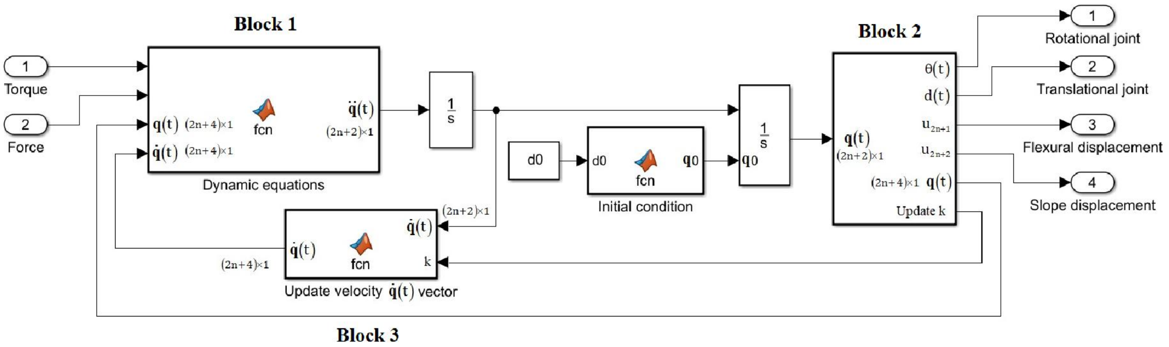

Fig. 3. Schematic solving differential equations in MATLAB/SIMULINK

Considering step i, the value $k(i)$ is calculated in Eq. (2). Size of $\mathbf{M}_{(i)},\mathbf{K}_{(i)},\mathbf{C}_{(i)}$ is $(2n+4)\times(2n+4)$ and $\mathbf{q}_{(i)},\mathbf{Q}_{(i)}$ is $(2n+4)\times1$. Declaration $\mathbf{M}^*_{(i)},\mathbf{K}^*_{(i)},\mathbf{C}^*_{(i)}$ with size is $(2n+2)\times(2n+2)$ and $\mathbf{q}^*_{(i)},\mathbf{Q}^*_{(i)}$ with size is $(2n+2)\times1$. Attaching elements of $\mathbf{M}_{(i)},\mathbf{K}_{(i)},\mathbf{C}_{(i)}$ to $\mathbf{M}^*_{(i)},\mathbf{K}^*_{(i)},\mathbf{C}^*_{(i)}$ with $k(i)$ variable is implemented at Block 1 (Fig. 3). Example with $\mathbf{M}^*_{(i)}$ matrix and $\mathbf{q}^*_{(i)},\mathbf{Q}^*_{(i)}$ vectors:

$$\begin{aligned}
&\mathbf{M}^*_{(i)}\left[1:(2k(i)+1);1:(2k(i)+1)\right]=\mathbf{M}_{(i)}\left[1:(2k(i))+1;1:(2k(i)+1)\right]\\
&\mathbf{M}^*_{(i)}\left[(2k(i)+2):(2n+2);(2k(i)+2):(2n+2)\right]=\mathbf{M}_{(i)}\left[(2k(i)+4):(2n+4);(2k(i)+4):(2n+4)\right]\\
&\mathbf{Q}^*_{(i)}\left[1:(2k(i)+1);1\right]=\mathbf{Q}_{(i)}\left[1:(2k(i))+1;1\right];\mathbf{q}^*_{(i)}\left[1:(2k(i)+1);1\right]=\mathbf{q}_{(i)}\left[1:(2k(i))+1;1\right]
\end{aligned} \tag{9}$$

The others matrices and vectors are operated the same way. Note that all of generalized matrices and vectors must be retrieved inertia size in step i+1 at Block 2 and Block 3 for calculating next step with updating $k(i+1)$ value.

3. CONTROLLER DESIGN

3.1. Control law

Elastic displacements at the end-effector effect on position accuracy of flexible robot. Therefore, control law must be designed to minimum reduced these influences. Considering the extended PID control law which includes reducing elastic displacement factor and is given as below

$$\xi(t)=\mathbf{K}_P e(t)+\mathbf{K}_D \dot{e}(t)+\mathbf{K}_I u(t)\int_0^t \dot{e}(s)u(s)ds \tag{10}$$

The previous PID controller which has not reducing elastic displacement factor is shown as

$$\xi(t)=\mathbf{K}_P e(t)+\mathbf{K}_D \dot{e}(t)+\mathbf{K}_I \int_0^t \dot{e}(s)ds \tag{11}$$

Where, $\mathbf{e}(t)=\begin{bmatrix}\theta_{ref}-\theta_{real} & d_{ref}-d_{real} & 0 & . & . & 0\end{bmatrix}^T$ is the joint variables error vector, $\xi(t)=\begin{bmatrix}\tau(t) & F(t) & 0 & . & . & 0\end{bmatrix}^T=\mathbf{Q}(t)$ is the applied force vector in Eq. (4), $u(t)=u_{2n+1}(t)$ is the elastic displacement at the end-effector, K_P, K_I, K_D are the zero matrix excepted positions $(1,1),(1,2)$ which are the values of control system. The size of $\mathbf{e}(t),\xi(t)$ is $(2n+4)\times 1$, size of K_P, K_I, K_D is $(2n+4)\times(2n+4)$. θ_{ref} and d_{ref} are the desired values and the input data. θ_{real} and d_{real} are the output data of control system. Lyapunov function V is given as $V=T+P+\frac{1}{2}\mathbf{e}^T\mathbf{K}_P\mathbf{e}+\frac{1}{2}\mathbf{K}_I\left[\int_0^t \dot{\mathbf{e}}(s)u(s)ds\right]^2$. Derivating of V is computed as $\dot{V}=\dot{T}+\dot{P}+\dot{\mathbf{e}}^T\mathbf{K}_P\mathbf{e}+\mathbf{K}_I\dot{\mathbf{e}}u(t)\int_0^t \dot{\mathbf{e}}u(s)ds$ with $\dot{T}+\dot{P}=\dot{\mathbf{q}}^T\left(\mathbf{M}\ddot{\mathbf{q}}+\frac{1}{2}\dot{\mathbf{M}}\dot{\mathbf{q}}+\mathbf{K}\mathbf{q}\right)=\dot{\mathbf{q}}^T\left(\xi(t)+\frac{1}{2}\dot{\mathbf{q}}\left(\dot{\mathbf{M}}-2\mathbf{C}\right)\right)$. Note that $\ddot{\mathbf{q}}^T\mathbf{M}\dot{\mathbf{q}}=\dot{\mathbf{q}}^T\mathbf{M}\ddot{\mathbf{q}}$ and $\dot{\mathbf{q}}^T\mathbf{K}\mathbf{q}=\mathbf{q}^T\mathbf{K}\dot{\mathbf{q}}$ with $\mathbf{M}$, $\mathbf{K}$ are the symatric matrices. So, $\dot{V}=-\dot{\mathbf{q}}^T\mathbf{K}_D\dot{\mathbf{q}}+\frac{1}{2}\dot{\mathbf{e}}^T\left(\dot{\mathbf{M}}\text{-}2\mathbf{C}\right)\dot{\mathbf{e}}\leq 0$ with $\dot{\mathbf{e}}^T\left(\dot{\mathbf{M}}\text{-}2\mathbf{C}\right)\dot{\mathbf{e}}=0$ because $\left(\dot{\mathbf{M}}\text{-}2\mathbf{C}\right)$ is the skew-matrix [17]. We can conclude that controller can achieve stable with control law in Eq. (10).

3.2. PSO algorithm

This paper presents the PSO algorithm to find the suitable parameters of the PID controller. Each particle moves about the cost surface with a velocity. The particles update their velocities and positions based on the local and global best solutions. Fig. 4 shows the movement of a single particle (i) at the time step $t(i)$ in space search. At time step $t(i)$, the position, velocity, personal best and global best are indicated as $x_i(t), v_i(t), p_i(t)$ and $p_g(t)$, respectively. The velocity $v_i(t)$ serves as a memory of the previous flight direction, can be seen as momentum. At time step $(t+1)$, the new position $x_i(t+1)$ can be calculated based on three components which are momentum, cognitive and social component [15].

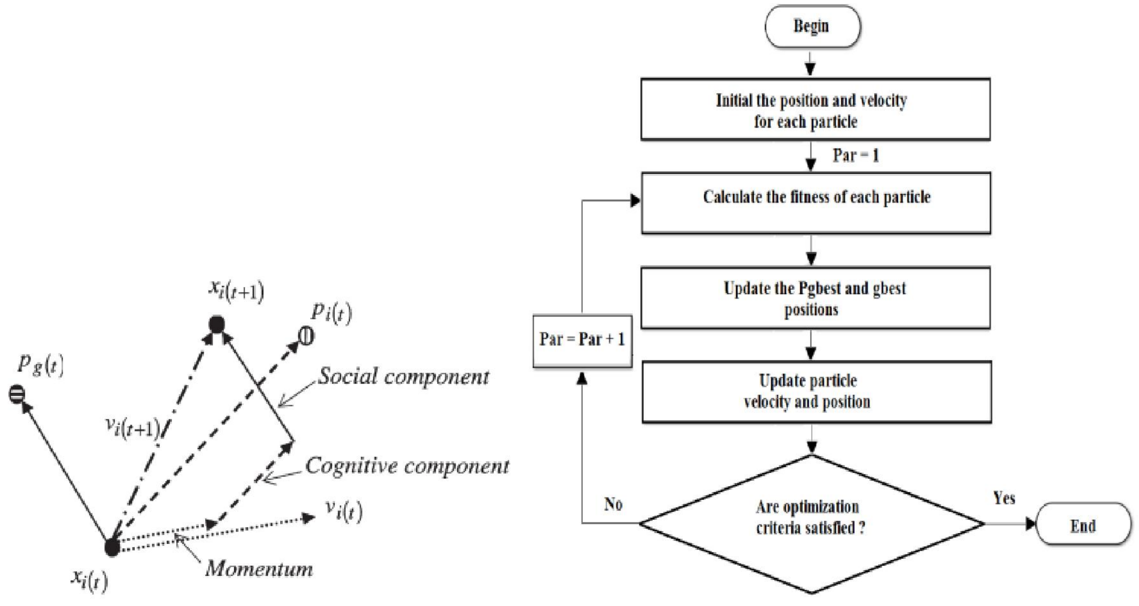
$x_i(t+1)$
$p_i(t)$
$p_g(t)$
Social component
$v_i(t+1)$
Cognitive component
$v_i(t)$
$x_i(t)$
Momentum
Begin
Initial the position and velocity for each particle
Par = 1
Calculate the fitness of each particle
Update the Pgbest and gbest positions
Par = Par + 1
Update particle velocity and position
No
Are optimization criteria satisfied ?
Yes
End

Fig. 4. The movement of a single particle and steps in PSO algorithm

After finding the personal best and global best, particle is then accelerated toward those two best values by updating the particle position and velocity for the next iteration using the following set of equations which are given as

$$\begin{aligned} &v_i(t)=kv_i(t-1)+C_1.\text{rand}.\left(P_i-x_i(t-1)\right)++C_2.\text{rand}.\left(P_g-x_i(t-1)\right); \\ &x_i(t)=x_i(t-1)+v_i(t); \end{aligned} \tag{12}$$

Where, C_1 and C_2 are learning factors. Symbol rand is the random number between 0 and 1. Symbol k is the inertia serves as memory of the previous direction, preventing the particle from drastically changing direction. The information details of PSO algorithm can be considered as. The sequences of operation in PSO are described in figure 4 with variable *par* are the optimum solution. The objective function $J=\int_0^{T_d}\left(\left(\mathbf{e}^*\right)^T\left(\mathbf{e}^*\right)+\xi^T\xi\right)dt$ is used in this study. Fitness function J is the linear quadratic regulator (LQR) function. Function J includes the sum-squared of error $\left(\mathbf{e}^*\right)$ of joints and elastic displacements and sum-squared of driving energy. The optimum target is finding the minimum cost of J function with values of respective parameters of PID controllers which are changed from lower bound to upper bound values.

4. NUMERICAL SIMULATION

In this work, simulation results are presented for two cases. Case 1 is reduced elastic displacement and case 2 is without reduced elastic displacement in joint space. Parameters of dynamic model, reference point and PSO algorithm are shown in Table. 1. It noted that values of lower and upper bound of variables are determined from auto tuning mode in MATLAB/SIMULINK.

Table 1. Dynamic configure of robot and PSO algorithm parameters

Parameters of flexible robot		**Parameters of PSO algorithm**	
Number of elements of link 2	n=5	Number of particles in a swarm	50
Length of link 1, link 2 (m)	L_1=0.2; L_2=0.8	Number of searching steps for a particle	50
Cross-section area (m^2)	A_1= 2.5x10^{-3}; A_2=4.5x10^{-5}	Cognitive and social acceleration	2
Mass of payload (kg)	m_t=0.1	Max and min inertia factor	0.9; 0.4
Mass density (kg/m^3)	$\rho_1=\rho_2=7850$	Number of optimization variables	6
Young's modulus (N/m^2)	$E_1=E_2=2\times10^{10}$	Lower bound of variables	0
Simulation time (seconds)	20	Upper bound of variables	10
Reference points	$\theta_{ref}=1.57(rad);d_{ref}=0.3(m)$		
The optimum parameters of PID with reducing elastic displacement (reduced): kp_1=5.84; kd_1=0.285; ki_1=1.897; kp_2=5.69; kd_2=1.97; ki_2=1.68 The optimum parameters of PID without reducing elastic displacement (not reduced): kp_1=7.88; kd_1=0.59; ki_1=1.42; kp_2=7.12; kd_2=7.89; ki_2=2.19			

The joint displacements, error control and deviation between both cases are shown in fig. 5 and fig. 6. Flexural and slope displacement at the end-effector are described in fig. 7 and fig. 8. Applied torque and force at joints is presented in fig 9 while deviation between them is shown in fig. 10. The simulation results in figures show that position accuracy in case reducing elastic displacement is higher than other case. Error of position is reduced about 10%. Setting time is reduced from 10(s) to 2(s) (fig. 6).

In general, simulation results show that initial control requests in jointspace are warranted with extended PID controller. The errors of joint variables are fast reduced. However, elastic displacements are not absolutely eliminated and these values effect on position of end-effector point in workspace.

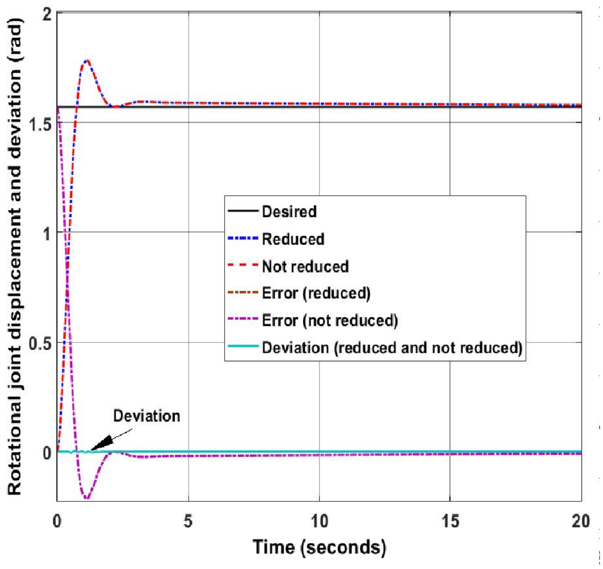

Fig. 5. Rotational joint displacement

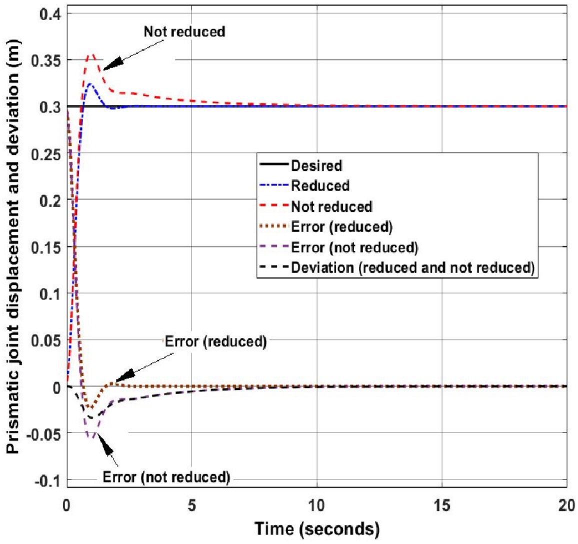

Fig. 6. Translational joint displacement

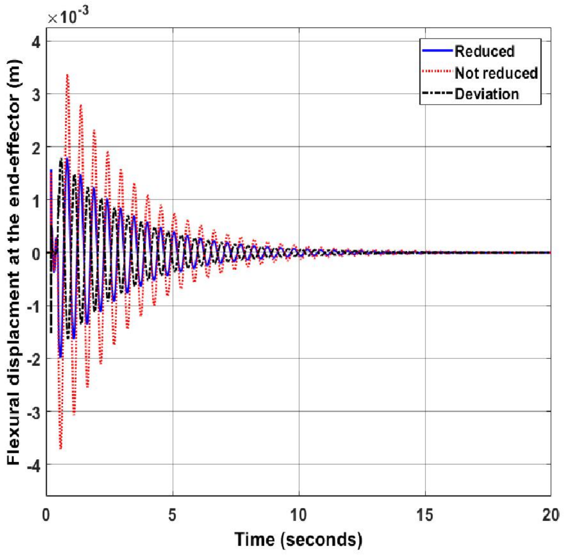

Fig. 7. Flexural displacement

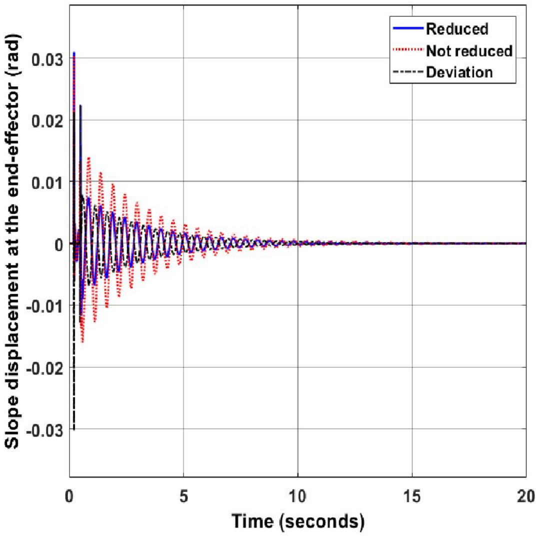

Fig. 8. Slope displacement

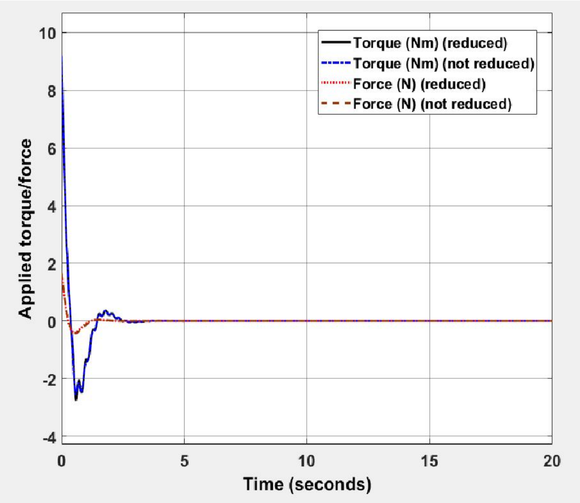

Fig. 9. Applied torque and force

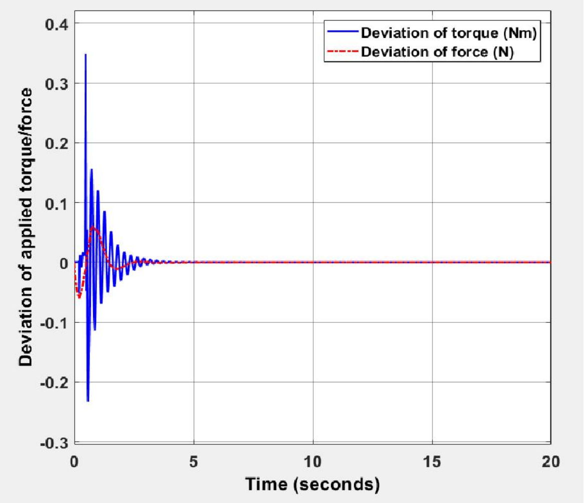

Fig. 10. Deviation applied torque/force

5. CONCLUSIONS

Designing extended PID controller of a flexible link robot combining rigid and flexible link, combining rotational and translational joint is presented. Equations of motion are built based on using finite element method and Lagrange approach. Extended PID control system is proposed to warrant following reference point in joint space. The position error is reduced based on reducing elastic displacement at the end-effector. Parameters of PID control are optimized by using PSO algorithm. The output search results are successfully applied to control position. The solving technique with changing conditions boundary also clealy presented.

ACKNOWLEDGMENT

This research is funded by Vietnam National Foundation for Science and Technology Development (NAFOSTED) under grant number 107.04-2017.09.

REFERENCES

[1]. Lochan, K., Roy, B. K. & Subudhi, B., 2016. A review on two-link flexible manipulators. *Annu. Rev. Control* **42,** 346–367.

[2]. Kiang, C. T., Spowage, A. & Yoong, C. K., 2015. Review of Control and Sensor System of Flexible Manipulator. *J. Intell. Robot. Syst. Theory Appl.* **77,** 187–213.

[3]. Sayahkarajy, M., Mohamed, Z. & Mohd Faudzi, A. A., 2016. Review of modelling and control of flexible-link manipulators. *Proc. Inst. Mech. Eng. Part I J. Syst. Control Eng.* **230,** 861–873.

[4]. Zhu, G., Lee, T. H. & Ge, S. S., 1997. Tip Tracking Control of a Single-Link Flexible Robot: A Backstepping Approach. *Dyn. Control* **7,** 341–360.

[5]. Yuh, J. & Young, T., 1991. Dynamic Modeling of an Axially Moving Beam in Rotation : Simulation and Experiment. *Trans. ASME* **113,** 34–40.

[6]. Pan, Y., Scott, R. A. & Ulsoy, A. G., 1990. Dynamic Modeling and Simulation of Flexible Robots With Prismatic Joints. *J. Mech. Des.* **112,** 307–314.

[7]. Ata, A. A., Fares, W. F. & Sa'Adeh, M. Y., 2012. Dynamic analysis of a two-link flexible manipulator subject to different sets of conditions. *Procedia Eng.* **41,** 1253–1260.

[8]. Al-Bedoor, B. O. & Khulief, Y. A., 1997. General Planar dynamics of a sliding flexible link. *J. Sound Vib.* **206,** 641–661.

[9]. Tokhi, M. O. & Azad, a. K. M., 2008. *Flexible Robot Manipulators*. The Institution of Engineering and Technology, London, United Kingdom.

[10]. Usoro, P. B., Nadira, R. & Mahil, S. S., 1986. A Finite Element/Lagrange Approach to Modeling Lightweight Flexible Manipulators. *J. Dyn. Syst. Meas. Control* **108,** 198–205.

[11]. Jalili, N., Xian, B. & Dawson, D. M., 2013. A Lyapunov-Based Piezoelectric Controller for Flexible Cartesian. *J. Dyn. Syst. Meas. Control* **126,** 347–358.

[12]. Khadem, S. E. & Pirmohammadi, A. A., 2003. Analytical development of dynamic equations of motion for a three-dimensional flexible link manipulator with revolute and prismatic joints. *IEEE Trans. Syst. Man, Cybern. Part B Cybern.* **33,** 237–249.

[13]. Kuo, K. Y. & Lin, J., 2002. Fuzzy logic control for flexible link robot arm by singular perturbation approach. *Appl. Soft Comput.* **2,** 24–38.

[14]. Khairudin, M. & Arifin, F., 2012. NN robust based-PID Control of A Two-Link Flexible Robot Manipulator. *Int. J. Adv. Sci. Eng. Inf. Technol.* **2,** 7–12.

[15]. Bahru, J., 2014. Self-tuning Active Vibration Controller using Particle Swarm Optimization for Flexible Manipulator System 2 Simulation of Flexible Manipulator Structure. *Trans. Syst. Control* **9,** 55–66.

[16]. Group, E. E., Branch, L. & Street, S., 2011. Backstepping method for a single-link flexible-joint manipulator using genetic algorithm. *Internatonal J. Innov. Comput. Int. Control* **7,** 4161–4170.

[17]. Lewis, F. L., 2004. *Manipulator Control Theory and Practice*. Marcel Dekker, Inc, USA.